Available online at www.sciencedirect.com
SCIENCE DIRECT
Materials Chemistry and Physics 92 (2005) 104–111
MATERIALS CHEMISTRY AND PHYSICS
www.elsevier.com/locate/matchemphys

Morphology evolution of anatase TiO_2 nanocrystals under a hydrothermal condition (pH = 9.5) and their ultra-high photo-catalytic activity

Churl Hee Cho[a,*], Moon Hee Han[a], Do Hyeong Kim[b], Do Kyung Kim[c]

[a] *Functional Materials Research Center, Korea Institute of Energy Research, 71-2 Jang-dong, Yusong-gu, Taejon 305-343, Republic of Korea*
[b] *Inorganic Materials Laboratory, Research Institute of Industrial Science and Technology, 32 Hyoja-dong, Pohang 790-330, Republic of Korea*
[c] *Department of Materials Science and Engineering, Korea Advanced Institute of Science and Technology, 373-1 Kusong-dong, Yusong-gu, Taejon 305-701, Republic of Korea*

Received 6 October 2004; received in revised form 10 December 2004; accepted 27 December 2004

Abstract

Morphology evolution of anatase TiO_2 nanocrystals under a hydrothermal condition (pH = 9.5) was observed and a relationship between the morphology evolution and photo-catalytic activity was investigated. A titanium hydroxide nanogel was neutrally precipitated from a $TiCl_4$ aqueous solution and then used as the precursor in the hydrothermal process. In the hydrothermal process, the nanogel was finally crystallized and grew to a capped bipyramidal nanocrystal which has faceted {1 0 1} pyramidal faces and are capped with rounded (0 0 1) faces, passing through an elongated structure with zigzag {1 0 1} faces. The final morphology was evolved via four growth stages in series: (i) formation and growth of anatase nuclei with consuming the nanogel, (ii) rapid growth along [0 0 1] direction by oriented attachments between (0 0 1) faces to produce an elongated structure with zigzag {1 0 1} pyramidal faces, (iii) flattening of zigzag {1 0 1} pyramidal faces by solution and precipitation, and (iv) rapid growth along [0 0 1] direction by solution and precipitation (Ostwald ripening). The photo-catalytic activity of anatase nanocrystals was closely related to the morphology evolution. Especially, the capped bipyramidal nanocrystals in the last growth stage showed an excellent photo-catalysis behavior: some of them were more than three times active than a commercial photo-catalyst (P25). The ultra-high photo-catalytic activity originated in the well-developed {1 0 1} surfaces, since the 4-coordinated Ti ions in the step edge of {1 0 1} face effectively adsorbed hydroxyl ions. Therefore, the particle morphology (surface property) was important as much as the particle diameter in TiO_2 photo-catalysis.

Keywords: Anatase nanocrystal; Hydrothermal growth; Morphology evolution; Photo-catalytic activity; 4-Coordinated Ti ions on {1 0 1} surface

1. Introduction

Anatase TiO_2 nanocrystals have attracted much attention due to high potentials applicable to photo-catalysts, catalyst supports, dye-sensitized electrode, and oxygen and humidity sensors. In all the applications, the diameter of anatase nanocrystals has been one of the most noticed materials parameters, since it directly affected the number of active sites (surface area) and electronic structure (size quantization). In recent years, there were a few research reports, announcing that anatase morphology (surface property) might play an important role in application property as much as the diameter [1,2]. Cho and coworkers have prepared spherical agglomerates of anatase nanocrystals by hydrothermal process and then reported the excellent photo-catalysis behavior [1]. It was suggested that the excellent photo-catalytic activity be related to the well-developed surfaces, easy to adopt hydroxyl ions. Also, one of interesting findings was that the photo-catalytic activity showed an abrupt increasing behavior as hydrothermal conditions were intensified, even though the diameter of primary anatase nanocrystals increased.

* Corresponding author. Tel.: +82 42 860 3505; fax: +82 42 860 3133.
E-mail address: chcho@kier.re.kr (C.H. Cho).

0254-0584/$ – see front matter © 2005 Elsevier B.V. All rights reserved.
doi:10.1016/j.matchemphys.2004.12.036

Hydrothermal process has been a promising route to synthesize anatase TiO_2 nanocrystals from titanium salts or titanium alkoxides, since it is able to produce defect-free nanocrystals with well-developed surfaces. Therefore, it is interesting to investigate how anatase nanocrystals get into a final shape in hydrothermal process. However, there were few research reports announcing morphology evolution of anatase nanocrystals in hydrothermal process [3,4]. Banfield and coworkers have systematically studied the morphology evolution of anatase nanocrystals during the hydrothermal crystallization in acidic or neutral aqueous solutions. Therefore, it is interesting to know how application properties such as photo-catalytic activity depend on the morphology evolution.

In the present study, anatase TiO_2 nanocrystals were prepared in a hydrothermal condition (pH = 9.5) and the morphology evolution was carefully observed by XRD and electron microscopy analysis. As an application property, the bulk and chemical activities were evaluated in a chloroform photocatalysis reaction. From the investigations, it was known that the photo-catalytic activity was highly dependent on the morphology evolution and the {1 0 1} surface is more active than (0 0 1) surface, since the 4-coordinated Ti ions in the stepped edge of {1 0 1} surface make a decisive role in the adsorption of hydroxyl ions. Therefore, it was concluded that the particle morphology (surface property) was important as much as the particle diameter in TiO_2 photo-catalysis.

2. Experimental

A titanium hydroxide nanogel was synthesized by neutral precipitation of titanium tetrachloride and then applied to the precursor of hydrothermal process to prepare anatase nanocrystals. Titanium tetrachloride ($TiCl_4$, 99.9%, Aldrich Chemical Co. Ltd., USA) was diluted with cold DI water to be a 0.3 M $TiCl_4$ aqueous solution. The 0.3 M $TiCl_4$ aqueous solution was transparent and its pH value was around 1. To prepare a titanium hydroxide nanogel, the 0.3 M $TiCl_4$ aqueous solution with a volume of 50 ml was vigorously mixed with a 7 ml of NH_3 aqueous solution (NH_3 28%, Junsei Chemical Co. Ltd., Japan). As soon as the NH_3 aqueous solution was introduced, the 0.3 M $TiCl_4$ aqueous solution got white and white, because a titanium hydroxide nanogel formed. After the neutral precipitation, the nanogel dispersion was strongly alkaline and its pH value was around 12. The nanogel was three times water washed by a combined process of centrifugation and dispersion to get rid of chlorine ions. After the water washing process, the nanogel was well dispersed in a 70 ml of DI water. The pH value of the nanogel dispersion was around 9.5, still strongly alkaline.

The nanogel dispersion with a volume of 70 ml was installed into a teflon-lined stainless steel mini-autoclave with an internal volume of 100 ml, and then the mini-autoclave was carried in a preheated convection oven to crystallize the nanogel under the hydrothermal condition. After the hydrothermal crystallization, the prepared titania nanocrystals were three times water washed by a combined process of centrifugation and dispersion. The wet titania nanocrystals were again dispersed in a 100 ml of DI water and then dried in a convection oven at 110 °C during a couple of overnights. After the evaporation drying, the dried titania nanocrystals were weakly agglomerated each others, so that they were well dispersed in DI water or ethyl alcohol by simple hand-grinding and then sonication processes.

Morphology of titania nanocrystals was investigated by electron microscopies (TEM and SEM). A small amount of titania nanocrystal was well dispersed in pure ethyl alcohol by sonication process. A TEM specimen was prepared by dipping up the nanocrystal dispersion with a carbon film-coated 200 mesh copper grid. In the TEM analysis, the morphology of titania nanocrystal was observed in bright field and high resolution modes, and ED pattern was applied for surface identification. Three-dimensional morphology of titania nanocrystal was observed by field-emission SEM analysis.

Crystalline phase, average diameter and fraction of crystallization of titania nanocrystals were identified by X-ray diffraction (XRD) analysis. Average diameters of anatase nanocrystal along [1 0 0], [0 0 1] and [1 0 1] crystallographic directions were calculated by Scherrer formula calibrated with Warren method [5]. In the diameter calculations along [1 0 0], [0 0 1] and [1 0 1] directions, (2 0 0), (0 0 4) and (1 0 1) diffraction peaks of anatase phase were used. Fraction of crystallization was evaluated by using a relative integral intensity of anatase (1 0 1) diffraction peak, since the integral intensity is directly proportional to the fraction of crystallization. Generally, this evaluation method has been used to study the crystallization and phase transformation of titania under hydrothermal conditions [6]. In the XRD analysis to evaluate the diameter and the fraction of crystallization, a commercial anatase particle (99.9%, Aldrich Chemical, Milwaukee, WI) with an average diameter of 0.2 μm was used as a reference sample.

Specific surface area of titania nanocrystals was evaluated by BET analysis with three point method. Before the BET analysis, titania nanocrystals were dried at 120 °C during overnight and then out-gassed at 200 °C for 3 h. UV transmissions of titania nanocrystals were evaluated by UV–vis–IR analysis to investigate energy band structure and calculate photo-catalytic activity. Photo-catalytic activity of titania nanocrystals was estimated by monitoring chlorine ions generated in the chloroform, a representative chlorinated hydrocarbon, photo-catalysis. The detailed evaluation process of photo-catalytic activity has been reported elsewhere [1].

3. Results and discussion

3.1. Morphology evolution of anatase nanocrystals

A titanium hydroxide nanogel, synthesized by neutral precipitation of titanium chloride, was used as a precursor

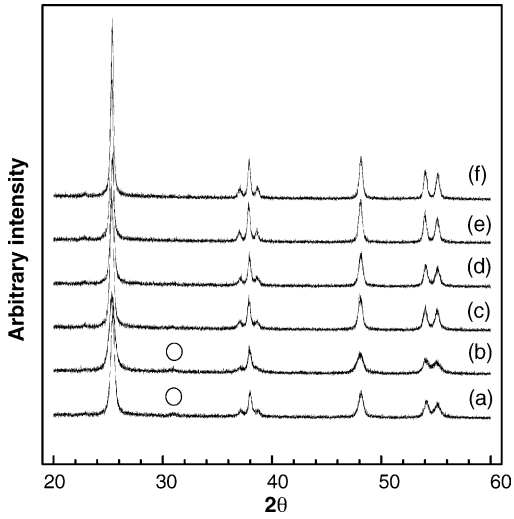

Fig. 1. XRD patterns of TiO_2 nanocrystals prepared by hydrothermal crystallization of nanogels at (a) 160 °C for 4 h, (b) 160 °C for 8 h, (c) 200 °C for 8 h, (d) 200 °C for 16 h, (e) 240 °C for 32 h and (f) 240 °C for 64 h. Ignorable brookite peaks (◯) were shown in the early stage of hydrothermal crystallization.

for hydrothermal process to prepare TiO_2 nanocrystals. XRD analysis showed that the nanogel was mainly composed of amorphous phase and contained a negligible amount of anatase nanocrystals with an average diameter of 3 nm. Fig. 1 represents XRD patterns for TiO_2 nanocrystals prepared by hydrothermal process. All the prepared TiO_2 nanocrystals were anatase form, even though ignorable brookite peaks were shown in anatase nanocrystals in the early stage of hydrothermal crystallization. In diameter calculations with XRD data, it was consistently shown that the average diameter along [1 0 0] direction got large and large with hydrothermal temperature and time increased. Hereinafter, the average diameter along [1 0 0] direction will be used as a measure of the degree of hydrothermal treatment.

TEM bright field images of the anatase nanocrystals prepared by hydrothermally crystallizing the nanogel at diverse conditions were represented in Fig. 2. It is remarkable that anatase nanocrystals do not grow equidimensionally in the hydrothermal solution. In an early stage of hydrothermal process, an elongated nanocrystal with zigzag surfaces appeared (Fig. 2(a)). The elongated nanocrystal looks like an agglomerate in which a few equidimensional nanocrystals stand in a line. In a late stage of hydrothermal process, anatase nanocrystals with well-developed faceted surfaces appeared (Fig. 2(f)). In the interior of the nanocrystal arrowed in Fig. 2(f), there was a void of which shape was well consistent with that of the nanocrystal. It means that the nanocrystal is a single crystal and well developed into an equilibrium shape under the hydrothermal condition.

Morphology evolution of anatase nanocrystals during the hydrothermal process was more clearly shown in the XRD

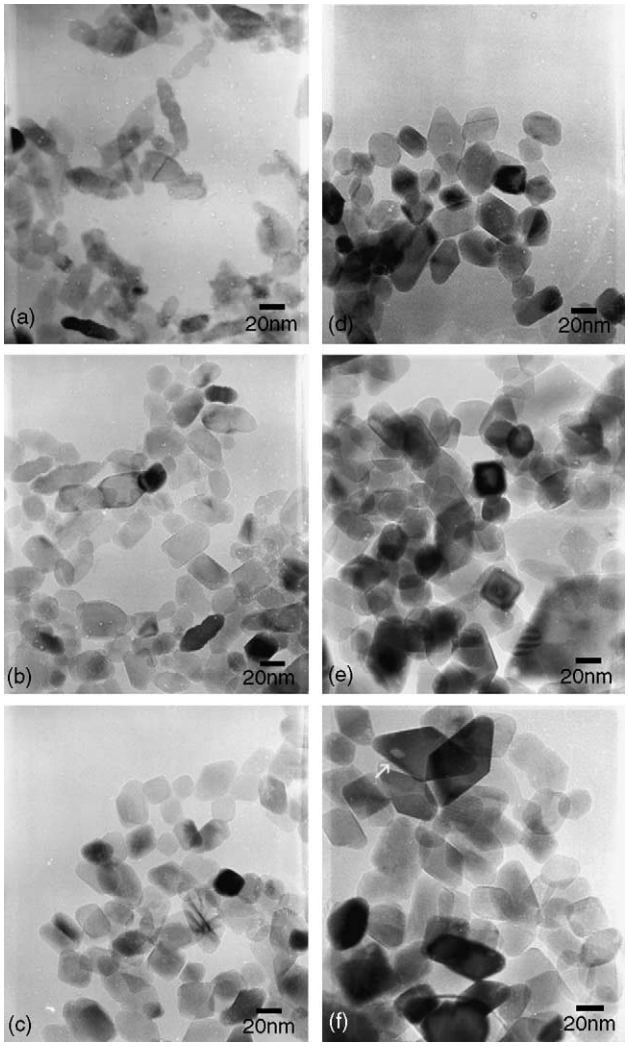

Fig. 2. TEM bright field images of anatase TiO_2 nanocrystals prepared by hydrothermal crystallization of nanogels at (a) 200 °C for 2 h, (b) 200 °C for 4 h, (c) 200 °C for 8 h, (d) 200 °C for 16 h, (e) 240 °C for 32 h and (f) 240 °C for 64 h, respectively. In all cases, the pH value of hydrothermal aqueous solution was constant to be 9.5. The nanocrystal arrowed in Fig. 1(f) contained a well-developed void.

analysis data for the average diameters of anatase nanocrystals along [1 0 0], [1 0 1] and [0 0 1] directions (Fig. 3(a)). The growth of anatase nanocrystal in the hydrothermal solution occurred via four growth stages in series. In the first growth stage, small equidimensional anatase nanocrystals formed and grew. In the second growth stage, anatase nanocrystals grew abruptly along [0 0 1] direction. The third growth stage involves an acceleration along [1 0 1] direction and a retardation along [0 0 1] direction, so that the diameter along [0 0 1] direction becomes equal to that along [1 0 1] direction. In the final growth stage, the diameter along [0 0 1] direction grew more rapidly than that along [1 0 1] direction. This complex growth behavior was also shown in the XRD analysis data for the diameter ratio of along [0 0 1] to along [1 0 1] as a function of the diameter along [1 0 0] direction, a measure of the degree of hydrothermal treatment (Fig. 3(b)).

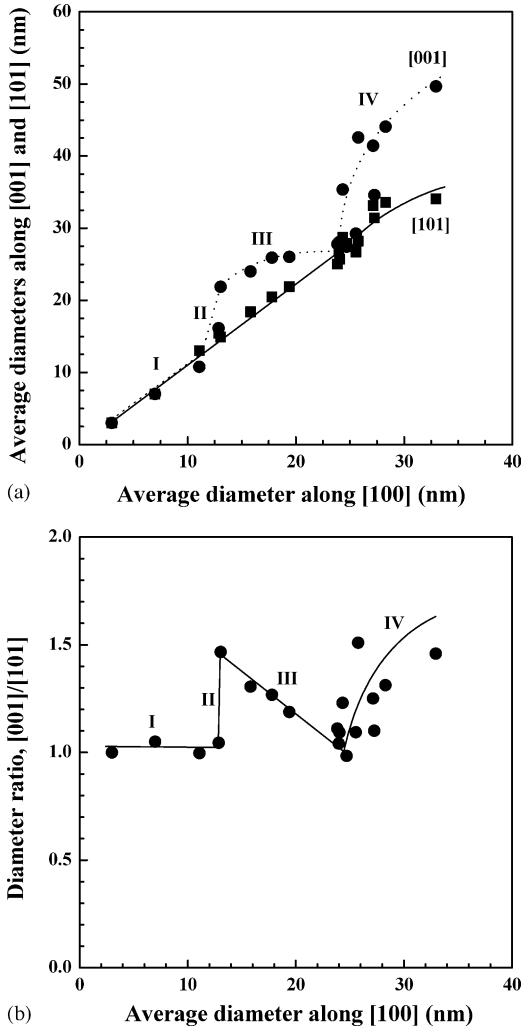

Fig. 3. Graphs of (a) average diameters along [0 0 1] and [1 0 1] directions and (b) diameter ratio of along [0 0 1] to along [1 0 1] of anatase nanocrystals as a function of the average diameter along [1 0 0] direction. The average diameter in each crystallographic direction was calculated by Scherrer formula from XRD data.

Banfield and coworkers have reported similar results for the hydrothermal growth of anatase nanocrystals in acidic or neutral condition [3]. In their data, hydrothermal time was used as a horizontal axis. Under the hydrothermal conditions, a rapid growth occurs along [0 0 1] direction, driven in part by the relatively high surface energy of (0 0 1) surface and in part by a kinetic effect involving a cyclic generation of highly reactive adsorption sites. The rapid growth along [0 0 1] direction depresses the growth rate along [1 0 1] direction, until (0 0 1) surfaces shrink to a constant cluster size. In their report, a second coarsening mechanism, oriented attachment, was clearly observed and activated when the pH of the hydrothermal solution decreased to 3 [3,4]. In Figs. 2(a) and Fig. 3, the second coarsening mechanism was seen dimly, since the anatase nanocrystals were hydrothermally grown in a strong alkaline aqueous solution (pH = 9.5). The strong alkalinity made solution-precipitation mechanism to get more activated, so that as shown in Fig. 2(a), the zigzag surfaces of the elongated nanocrystals were already flattened to some extent.

HRTEM images and ED patterns of the anatase nanocrystals prepared by hydrothermal crystallization of the nanogel at (a) 200 °C for 2 h, (b) 200 °C for 32 h and (c) 240 °C for 64 h were represented in Fig. 4. The anatase nanocrystals shown in Fig. 4(a) and (b) were in the third growth stage, and that shown in Fig. 4(c) was in the final growth stage. HRTEM and ED data showed that in the faceted nanocrystal, the flat faces were {1 0 1} surfaces and the rounded faces were (0 0 1) surfaces, and the zigzag surfaces shown in Fig. 4(a) and (b) were {1 0 1} faces which were flattened in the third growth stage.

Generally, morphology evolution of a crystal in gas or liquid phase is determined by the driving force of the further reduction in energy due to minimization of the area of high surface energy faces, because the effect of strain energy is ignorable [7]. Therefore, it is important to know which surface is more stable energetically and what kind of equilibrium shape is plotted by a Wulff construction. From a view-point of thermodynamics, rutile is more stable than anatase. Anatase nanocrystals exist in a metastable state, because its average surface energy is smaller than that of rutile. Since it is difficult to obtain sufficiently large and pure anantase crystals, experimental investigations on surface energy of anatase crystals are just starting and surface energy data were mostly dependent on model-based calculations. Classical Donnay–Harker rules predict that in an anatase crystal, the surface energy of the (0 0 1) face is approximately 1.4 times that of the {1 0 1} face [4]. Recently, Lazzeri and coworkers have published ab initio calculations on the structure and energetics of stoichiometric anatase surfaces. Using the density functional theory, they calculated the formation energies of the most common orientations of anatase, and found the energies for the relaxed surfaces (from lowest to highest) to rank as: (1 0 1) < (1 0 0) < (0 0 1) < (1 0 3) < (1 1 0). The calculated surface formation energies for (1 0 1), (1 0 0), (0 0 1), (1 0 3) and (1 1 0) surfaces were 0.44, 0.53, 0.90, 0.84, 0.93 and 1.09 J m^{-2}, respectively. Based on the calculations, they performed a Wulff construction of the equilibrium crystal shape and their result was shown in Fig. 5(a). It closely resembles the shape of naturally occurring anatase mineral specimens, in which the bipyramidal structure has exposed faces that are {1 0 1} and are capped with (0 0 1) faces [8–10]. A field-emission SEM image of the faceted nanocrystals shown in Fig. 2(f) was represented in Fig. 5(b). The faceted anatase nanocrystal has three-dimensionally a capped bipyramidal structure, resembling the shape of naturally occurring anatase mineral specimens. The capped bipyramidal structure was well shown in the nanocrystals arrowed in Fig. 5(b).

From a view-point of kinetics, crystal morphology will be defined by the slowest growing faces because the fastest growing faces shrink [7]. Basically, there are two types of atomic structure for solid/liquid interfaces. One is an atomically flat interface, described as smooth, faceted, or

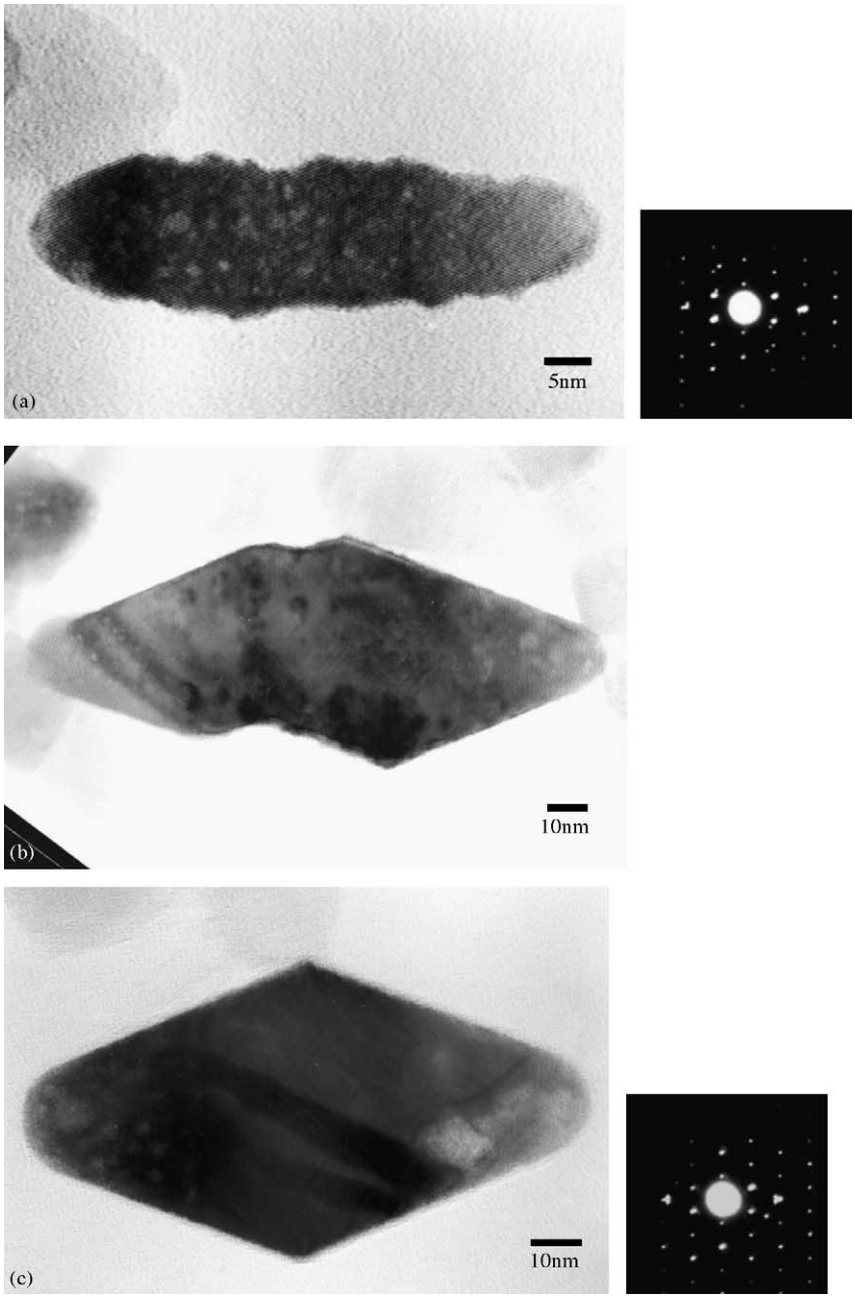

Fig. 4. HRTEM image and ED pattern of anatase nanocrystals. The anatase nanocrystals shown in (a) and (b) are in the third growth stage and one shown in (c) is in the fourth growth stage.

sharp, and the other is an atomically diffuse interface, known as rough or non-faceted. Generally, rough interfaces migrate by a continuous growth process while flat interfaces migrate by a lateral growth process involving ledges. Also, rough interfaces migrate much faster than flat interfaces. It is important to know the atomic structure of solid/liquid interface, because the growing velocity of solid/liquid interface was highly dependent on its atomic structure. Hebenstreit and coworkers have reported STM results and suggested a reasonable atomic model for anatase (1 0 1) surface [11]. The anatase (1 0 1) surface has only a pm symmetry, giving rise to a preferential orientation of step edges. In their model, titanium atoms at the terrace have 5-fold and 6-fold coordination, and titanium atoms at the step edge are 4-fold coordinated. It was suggested that these titanium atoms at the step edge have a higher reactivity against gas adsorption. Vittadini et al. and Lazzeri et al. have suggested reasonable atomic models for anatase (0 0 1) surface [12,13]. According to their models, the anatase (0 0 1) surface is atomically rough and exhibits 5-fold coordinated Ti atoms. The rough (0 0 1) surface was identified with a STM study by Tanner et al. [14]. In considering both surface energies and surface

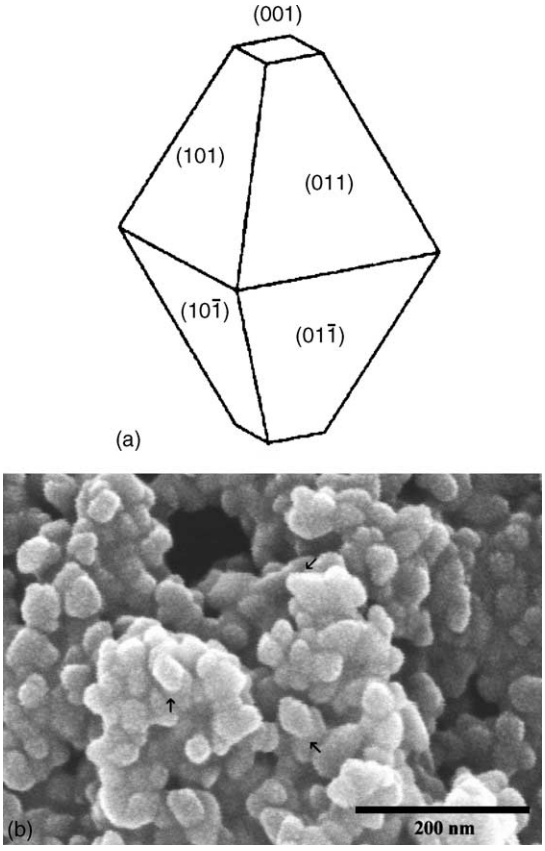

Fig. 5. (a) The equilibrium shape of an anatase crystal, according to the Wulf construction and surface energies calculated in [8] and (b) a FE-SEM image of the anatase nanocrystal shown in Fig. 1(f). The capped bipyramidal structure was well shown in the nanocrystals arrowed in Fig. 4(b).

structures of anatase, the flat anatase {1 0 1} surface with a small surface energy migrates more slowly than the rough (0 0 1) surface with a high surface energy. Therefore, anatase morphology will be defined by the slower growing {1 0 1} surfaces since the faster growing (0 0 1) face shrinks. As the capped bipyramidal nanocrystals in the fourth growth stage get large and large (grow), the area fraction of {1 0 1} surface will increase, while that of (0 0 1) surface will decrease.

A two-dimensional scheme for the morphology evolution of anatase nanocrystal in the hydrothermal condition (pH = 9.5) was represented in Fig. 6. In the first growth stage, an equidimensional anatase nanocrystal precipitates (nucleates and grows) with consuming the nanogel, since the nanogel has higher bulk energy, higher surface energy, and higher solubility than anatase crystals. In the second growth stage, the oriented attachments between anatase nanocrystals, firstly introduced by Banfield et al., abruptly enhanced the anisotrophic growth along the [0 0 1] direction. In the oriented attachment mechanism, the driving force is the reduction of total surface energy by eliminating high surface energy face with simple contacts. The oriented attachments occur between (0 0 1) faces with a high surface energy, and result in the elongated nanocrystals with the zigzag {1 0 1} surfaces as shown in Fig. 2(a). The oriented attachment

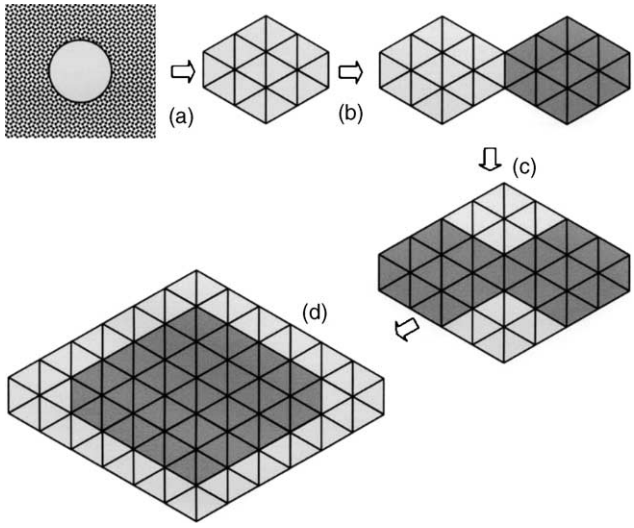

Fig. 6. A two-dimensional scheme for the growth of anatase nanocrystals under the hydrothermal condition (pH = 9.5). A capped bipyramidal anatase nanocrystals formed and grew via four growth stages in series: (a) gel dissolution and anatase precipitation, (b) orientation attachment between (0 0 1) surfaces, (c) {1 0 1} surface flattening by solution-precipitation and (d) rapid growth along [0 0 1] direction by solution-precipitation (Ostwald ripening).

mechanism is quite distinct from solution-precipitation mechanism, which involves the dissolution of fine particles or residual nanogels. The latter mechanism operates simultaneously with oriented attachment due to the high driving force for addition of ions from solution to newly formed crystal–crystal junctions, and governs the third growth stage which is concerned to the flattening phenomenon of the zigzag {1 0 1} surfaces. In the third growth stage, the diameter ratio of along [0 0 1] to along [1 0 1] decreases due to the high growth rate in the [1 0 1] direction by the flattening process. At the end of the third growth stage, a bipyramidal nanocrystals with faceted {1 0 1} surfaces and rounded (0 0 1) surfaces results in. Banfield and coworkers have suggested that the constant cluster size of the rounded (0 0 1) surface is ranged from 1.9 to 5.7 nm [3]. Their predicted cluster size of the rounded (0 0 1) surface is well consistent with the present result shown in Fig. 4(c). In the final growth stage, the bipyramidal nanocrystal grows by Ostwald ripening mechanism, consuming others. As shown in Fig. 3(a) and (b), when the fourth growth proceeds, the diameter ratio of along [0 0 1] to along [1 0 1] increases. It means that the area fraction of {1 0 1} surface increases, while the area fraction of (0 0 1) surface decreases in the fourth growth stage.

3.2. Relationship of morphology evolution to photo-catalytic activity

In the previous study [1], the authors have reported the photo-catalytic activity of the monodisperse spheroids synthesized by a combined process of thermal hydrolysis and hydrothermal crystallization. The monodisperse spheroids were composed of primary anatase nanocrystals and showed

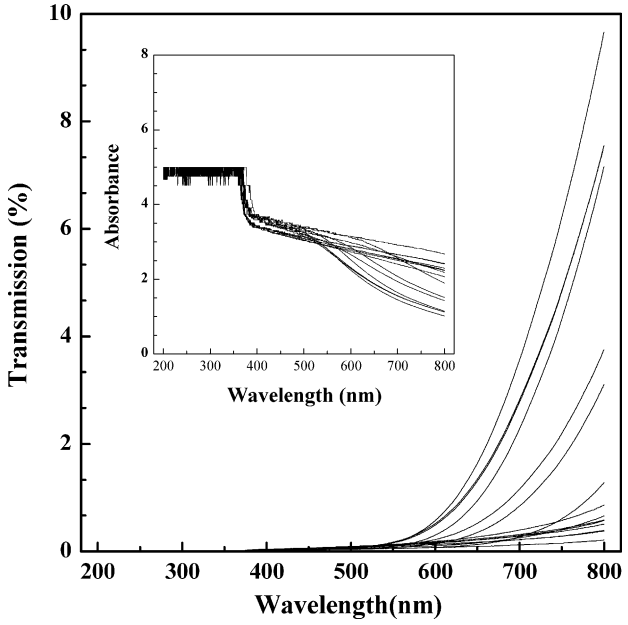

Fig. 7. Light transmission and absorption spectra for anatase aqueous dispersions used in chloroform photo-catalysis. In the aqueous dispersions, anatase concentration was 0.62 g l^{-1} and anatase diameter along [1 0 0] were ranged from 3 to 33 nm.

a good photo-catalysis behavior. The good photo-catalytic activity was closely related with its good surface adsorption ability for hydroxyl ions and then proven by the zeta-potential data: the anatase spheroids, prepared by hydrothermal process, had smaller isoelectric point than the calcined anatase and P25, a commercial photo-catalyst. Also, one of the interesting findings was that the photo-catalytic activity abruptly increased as the diameter of primary nanocrystals increased.

UV transmission is important because it informs energy band structure. Fig. 7 represents light transmission and absorption spectra for anatase aqueous dispersions used in chloroform photo-catalysis. In the aqueous dispersions, anatase concentration was 0.62 g l^{-1} and anatase diameter along [1 0 0] were ranged from 3 to 33 nm. All the anatase dispersions showed the same absorption behavior for UV lights: the absorption edge was around 395 nm, and the transmission at the UV light with a wavelength of 400 nm was 0.02–0.04% and independent of the anatase diameter. Generally, the size quantization effect, first reported by Anpo et al. and Zhang et al., is shown in the crystals with a diameter of less than 10 nm [15–17]. In the present study, the size quantization effect was not shown even in the anatase nanocrystals in the first growth stage. This means that all the prepared anatase nanocrystals have the same energy band structure. The same result was reported by Serpone et al. [18,19]. Also, it is remarkable that the transmission at the UV light with a wavelength of 400 nm was nearly independent of the anatase diameter. Therefore, in the present study, UV transmission was not considered in calculating photo-catalytic activity.

Bulk and chemical photo-catalytic activities of anatase nanocrystals were represented as a function of the average

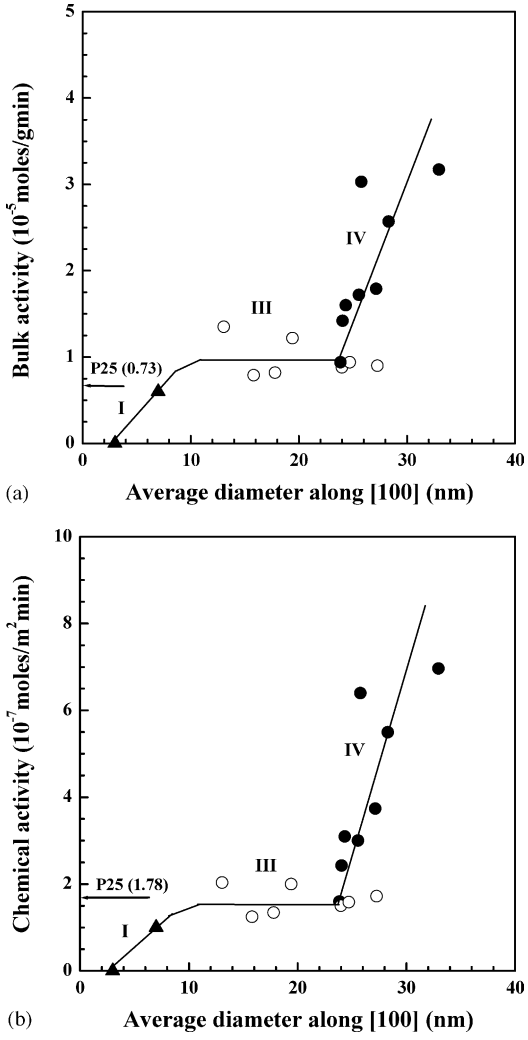

Fig. 8. (a) Bulk and (b) chemical photo-catalytic activities of the anatase nanocrystals in the (▲) first growth stage, (◯) third growth stage and (●) fourth growth stage as a function of average diameter along [1 0 0] direction. The photo-catalytic activity of P25, a commercial catalyst, was presented as a reference.

diameter along [1 0 0] direction in Fig. 8(a) and (b), respectively. When the average diameter along [1 0 0] direction increased, the photo-catalytic activities increased, saturated and sharply increased in series. The dependency of the photo-catalytic activity on the diameter along [1 0 0] direction, a measure of the degree of hydrothermal treatment, was closely related with the morphology evolution. In the first growth stage (anatase precipitation), the photo-catalytic activity increased as the diameter along [1 0 0] direction increased. The increment of photo-catalytic activity was explained by the increasing fraction of anatase nanocrystals, consuming the nanogel that is nearly inactive in photo-catalysis. In the third growth stages ({1 0 1} surface flattening), the photo-catalytic activity was nearly independent of the diameter along [1 0 0]. On the other hand, in the fourth growth stage, the photo-catalytic activity abruptly increased as the diameter along [1 0 0] direction increased. The abrupt increasing behavior of

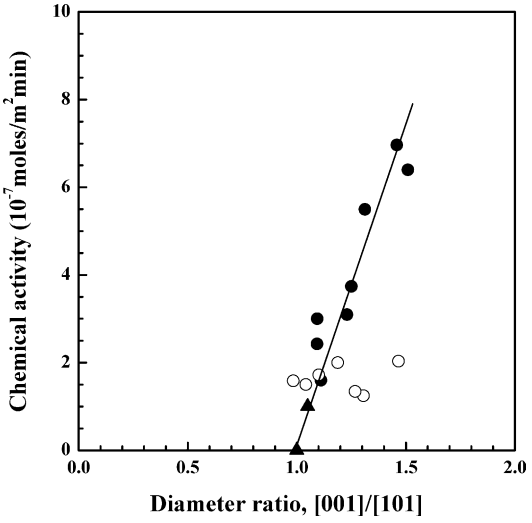

Fig. 9. Chemical photo-catalytic activity of the anatase nanocrystals in the (▲) first growth stage, (◯) third growth stage and (●) fourth growth stage as a function of the diameter ratio of along [0 0 1] to [1 0 1] directions. The diameter ratio is directly proportional to the area fraction of {1 0 1} surface in the fourth growth stage.

photo-catalytic activity in the fourth growth stage was more clearly shown in Fig. 9, representing the chemical photo-catalytic activity as a function of the diameter ratio of along [0 0 1] to along [1 0 1] directions. If the anatase nanocrystals in the third growth stages are not considered, the chemical activity of anatase nanocrystals increased linearly with the diameter ratio increased. The increment of the diameter ratio means the increment of the area fraction of {1 0 1} surface. Therefore, the {1 0 1} surface was more active than the (0 0 1) surface. The independence of photo-catalytic activity in the third growth stage could be explained, since there was no change of {1 0 1} surface fraction in the third growth stage.

Generally, the photo-catalytic activity in TiO_2 photo-catalysis was directly proportional to the number of surface hydroxyl radicals. The number of surface hydroxyl radicals is closely related to the concentration and coordination number of Ti ions on the surface. The {1 0 1} surface exhibits stepped structure with two types of 5-coordinated and one type of 4-coordinated Ti ions, while the {0 0 1} surface contains one type of 5-coordinated Ti ions. As the coordination number of Ti ion increases, the adsorption of negative-charged hydroxyl ions gets more difficult. The adsorption of hydroxyl ions will preferentially occur on the {1 0 1} surface with 4-coordinated Ti ions, so that the {1 0 1} surface is expected to be more active than the (0 0 1) surface. The expectation was well consistent with the experimental data (Figs. 8 and 9).

4. Conclusion

Anatase nanocrystal in a strong basic condition (pH = 9.5) grows to be a bipyramidal crystal, passing through an elongated structure. The morphology evolution was explained by a combined growth model: (i) nanogel dissolution and anatase precipitation; (ii) oriented attachment between (0 0 1) faces; (iii) {1 0 1} surface flattening by solution-precipitation; and (iv) rapid growth along [0 0 1] direction by solution-precipitation. The photo-catalytic activity of anatase nanocrystals was highly dependent on the morphology evolution. The bipyramidal anatase nanocrystal with the faceted {1 0 1} pyramidal faces and the rounded (0 0 1) capped face showed an excellent photo-catalytic behavior: some of them were more than 3 times that of P25, a commercial photo-catalyst. The {1 0 1} surface was more active than the (0 0 1) surface, since the 4-coordinated Ti ions in the stepped edge of {1 0 1} surface made a decisive role in the adsorption of hydroxyl ions. Therefore, the particle morphology (surface property) is known to be important as much as the particle diameter in TiO_2 photo-catalysis.

Acknowledgements

The present work was financially supported in part by the Research Institute of Industrial Science and Technology (RIST) and in part by the Center for Nanostructured Materials Technology (CNMT), Korea.

References

[1] C.H. Cho, D.K. Kim, D.H. Kim, J. Am. Ceram. Soc. 86 (2003) 1138.
[2] K.L. Yeung, S.T. Yau, A.J. Maira, J.M. Coronado, J. Soria, P.L. Yue, J. Catal. 219 (2003) 107.
[3] R.L. Penn, J.F. Banfield, Geochim. Cosmochim. Acta 63 (1999) 1549.
[4] R.L. Penn, J.F. Banfield, Amer. Miner. 83 (1998) 1077.
[5] B.D. Cullity, Elements of X-ray Diffraction, Addison-Wesley Publishing Co. Inc., Reading, MA, 1978.
[6] K. Yanagisawa, Y. Yamamoto, Q. Feng, N. Yamasaki, J. Mater. Res. 13 (1998) 825.
[7] D.A. Porter, K.E. Easterling, Phase Transformations in Metals and Alloys, Van Nostrand Reinhold Company Ltd., Berkshire, England, 1981.
[8] M. Lazzeri, A. Vittadini, A. Selloni, Phys. Rev. B 63 (2001) 155409.
[9] M. Lazzeri, A. Vittadini, A. Selloni, Phys. Rev. B 63 (2002) 119901(E).
[10] Ulrike Diebold, Surf. Sci. Rep. 48 (2003) 53.
[11] W. Hebenstreit, N. Ruzycki, G.S. Herman, Y. Gao, U. Diebold, Phys. Rev. B 62 (2000) R16334.
[12] A. Vittadini, A. Selloni, F.P. Rotzinger, M. Grätzel, Phys. Rev. Lett. 81 (1998) 2954.
[13] M. Lazzeri, A. Selloni, Phys. Rev. Lett. 87 (2001) 266105.
[14] R.E. Tanner, J. Phys. Chem. B 106 (2002) 8211.
[15] M. Anpo, T. Shima, S. Kodama, Y. Kubokawa, J. Phys. Chem. 91 (1987) 4305.
[16] C. Wang, Z. Zhang, J.Y. Ying, Nanostr. Mater. 9 (1997) 583.
[17] Z. Zhang, C. Wang, R. Zakaria, J.Y. Ying, J. Phys. Chem. B 102 (1998) 10971.
[18] N. Serpone, D. Lawless, R.J. Khairutdinov, J. Phys. Chem. 99 (1995) 16646.
[19] N. Serpone, D. Lawless, R. Khairudinov, E. Pelizzetti, J. Phys. Chem. 99 (1995) 16655.